REPORT 3A

# Simulations of the GBT Antenna with LQG Controller

by

**Wodek Gawronski and Ben Parvin**

August 23, 1995

## 1. Introduction

The preliminary analysis of the GBT antenna with LQG controller is presented. The LQG controller was designed and tested at the 34-m beam-waveguide antennas at Goldstone, CA. It had good tracking and vibration damping properties, as reported in [1], [2]. However, the wind disturbance rejection properties have not yet been tested. It was expected that the pointing (tracking) accuracy of the LQG controller in wind would be improved when compared with the PI controller.

## 2. LQG controller configuration

The block diagram of the antenna with the LQG controller is given in Fig.1. Besides the conventional PI part (with gains $k_p$, and $k_i$) it includes the estimator, which recovers the estimated states, $\hat{x}$, of the antenna states, $x$, using encoder measurements $y$ and the rate input $u$. The states, which simulate the antenna vibrations, are amplified by the gain vector $k_f$, such that the plant vibrations are suppressed.

The controller performance depends greatly on (1) the estimator accuracy, (2) the controller gains (proportional, $k_p$, integral, $k_i$, and modal, $k_f$).

The estimator gives the estimates of the unmeasured variables, such as modal displacement and rates. It should recover accurately the antenna dynamics during its operational time. For the simulation purposes the analytical model of the antenna at 60 deg elevation is used as estimator. However, it cannot be used as estimator of the "real" antenna. The discrepancy between the analytical model and the actual structure is significant enough to cause the instability of the closed-loop system. In order to assure the estimator precision, a model which is based on the actual antenna measurements should be used.

The other question is the non-uniqueness of the antenna model, specially for the azimuth motion, and its usefulness as estimator. When considering the azimuth model, one can see that the structure configuration changes, depending on the elevation position, see Fig.2, and the structural properties change with elevation angle. Indeed, from this figure the structure at 60 deg elevation will have some modes and frequencies different than the structure at 5 deg elevation. If one decides to use the antenna estimator determined at, say, 45 deg elevation, the question arises if this estimator is robust enough for the antenna at 90 deg elevation position. The tests of the LQG controller for the DSN antennas showed that it was robust to these variations. However, the GBT antenna is different than the fully symmetrical DSN ones, and the answer to this question cannot be found off-hand.

The LQG gains were determined using the procedure given in Ref.[1]. It assigns weights and consequently gains for each mode separately, allowing to check the performance of each individual mode.

## 3. Simulation results

The LQG controller response to the step command was simulated and compared to the step response of the PI controller, which was reported earlier, in GBT Memo 129. Figs.3a,b show the azimuth encoder and cross-elevation pointing response to the azimuth step command. They show the improved damping of the azimuth encoder and cross-elevation pointing oscillations, when compared to the PI controller. Similar situation is observed for the elevation encoder and elevation pointing response to the elevation step command, as in Figs.4a,b.

The LQG improved damping properties are also visible in the transfer functions plots: from azimuth command to azimuth encoder (Fig.5a), from azimuth command to cross-elevation pointing (Fig.5b), from elevation command to elevation encoder (Fig.6a), and from elevation command to elevation pointing (Fig.6b). The resonance peaks have been flattened, expanding the

antenna bandwidth, and improving tracking properties.

The wind disturbances rejection by the LQG controller are shown in Table 1 and compared with the PI controller.

Table 1. Pointing errors rms in arcsecs, for 50 mph wind gusts

| | PI front | PI side | LQG front | LQG side |
|---|---|---|---|---|
| cross-elevation pointing | 0.0 | 83.0 | 0.0 | 77.0 |
| elevation pointing | 13.0 | 3.5 | 1.2 | 3.0 |

The table shows almost the same pointing error for the PI and the LQG controllers. We cannot explain this fact at this moment, further study should be conducted to find the improved performance of the LQG controller in wind. It shall be noted, however, that the LQG controller is designed to improve the command following rather than the minimization of the errors caused by wind disturbances. Thus the design approach will be further evaluated and modified to find a better solution.

Figs.7a,b show the response of the azimuth encoder and cross-elevation beam to the side wind, and Figs.8a,b show the response of the elevation encoder and elevation beam to the front wind. Both figures show that the LQG controller mostly compensated for the higher frequency disturbances, leaving the low frequency disturbances, which are the most troublesome, almost untouched.

## Conclusions

The simulations of the GBT antenna with LQG controller show improvement in command following (much better vibration damping), and insignificant improvement in pointing in wind gusts. The simulations were performed without feed-forward loop (its addition improves the command following, but not the tracking in wind), and without imposed rate and acceleration limits.

## References


1. Gawronski, W., and J.A. Mellstrom, "Control and Dynamics of the Deep Space Network Antennas," a chapter in *Control and Dynamic System,* vol.63, ed. C.T. Leondes, Academic Press, San Diego, CA, 1994.
2. Gawronski, W., Racho, C., and Mellstrom, J.A., "LQG and Feedforward Controllers for the Deep Space Network Antennas," *IFAC Symposium on Automatic Control in Aerospace,* Palo Alto, CA, 1994.

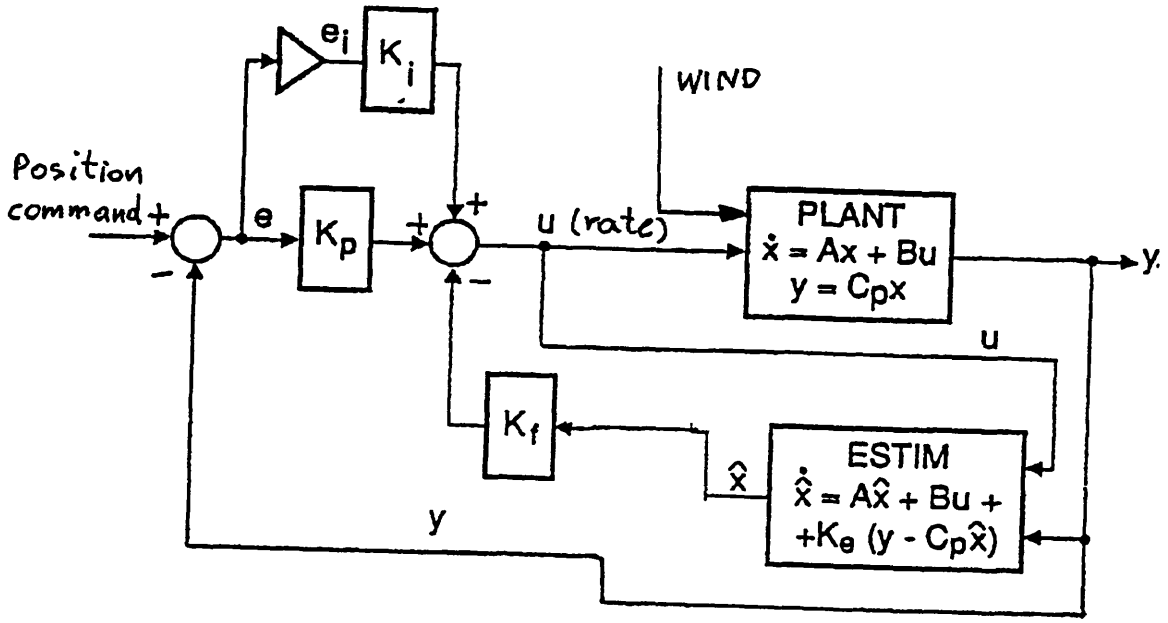


Fig.1. The block diagram of the antenna with the LQG controller

Fig.1

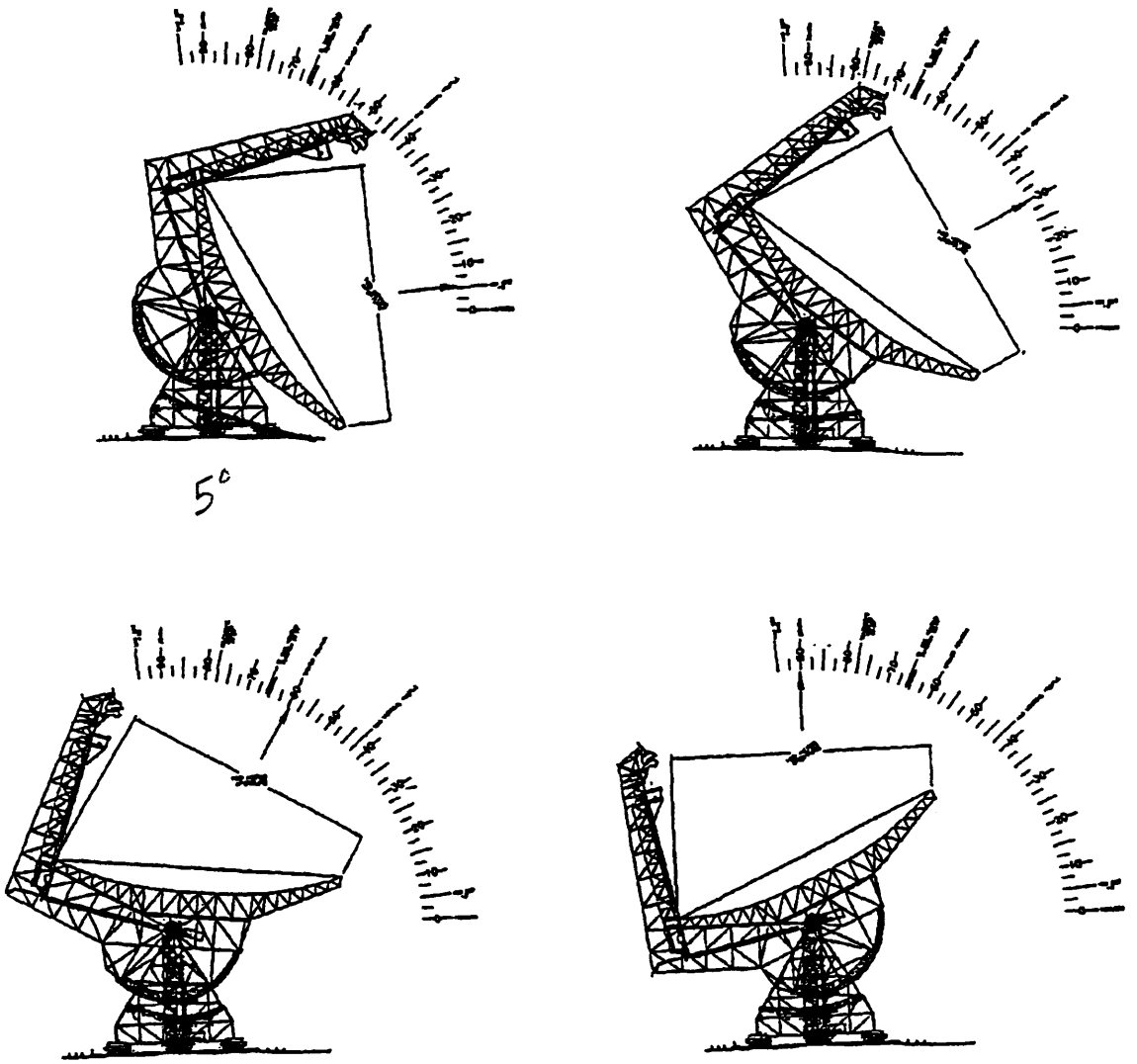


Fig.2. Antenna configuration for different elevation angles: (a) elevation angle=5deg, (b) elevation angle=30 deg, (c) elevation angle=60 deg, and (d) elevation angle=90 deg.

Fig.2a,b,c,d

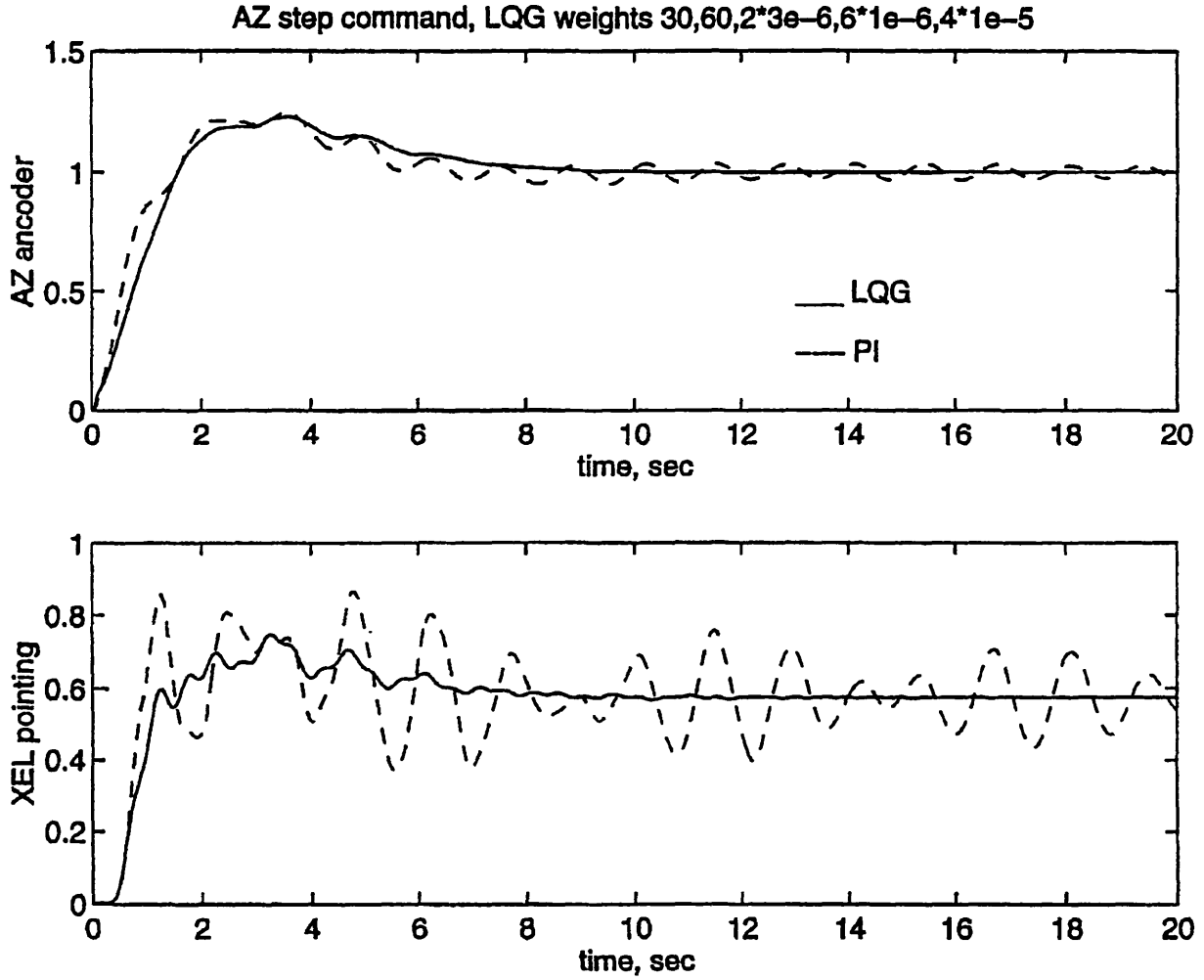


Fig.3 Azimuth encoder (a) and cross-elevation pointing (b) response to the azimuth step command.

Fig.3a,b

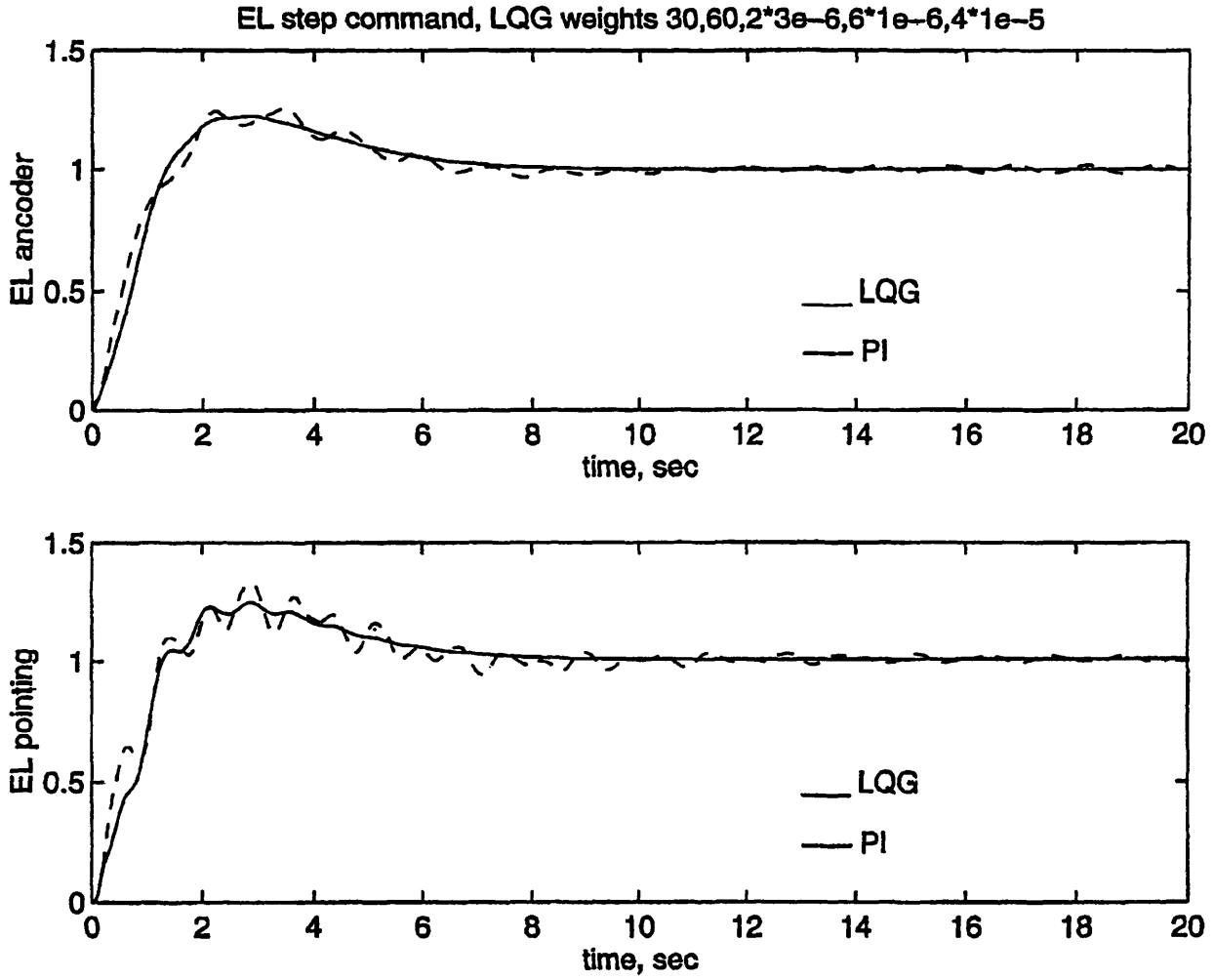


Fig.4 Elevation encoder (a) and elevation pointing (b) response to the elevation step command.

Fig.4a,b

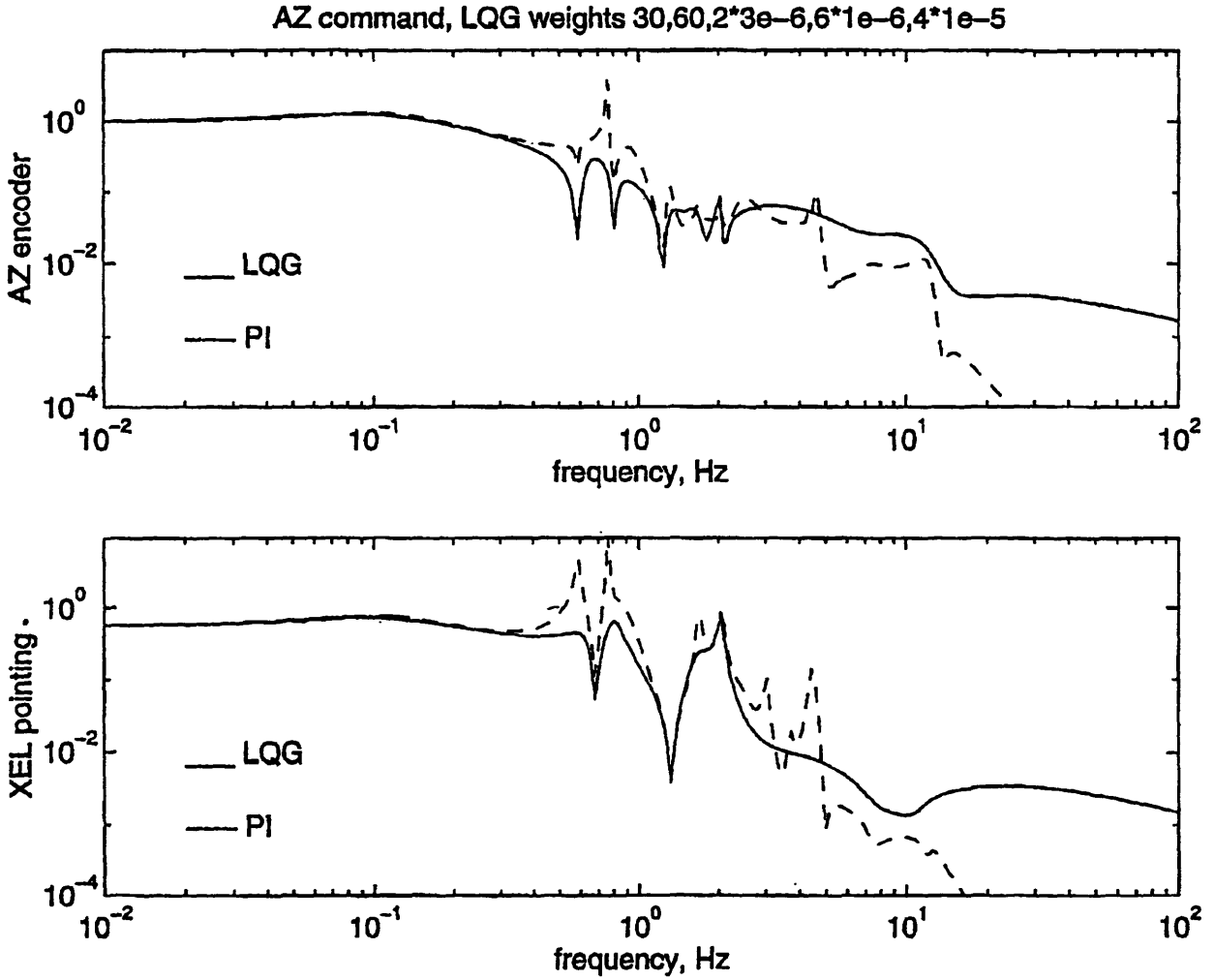


Fig.5 Magnitudes of transfer function: (a) from azimuth command to azimuth encoder, and (b) from azimuth command to cross-elevation pointing.

Fig.5a,b

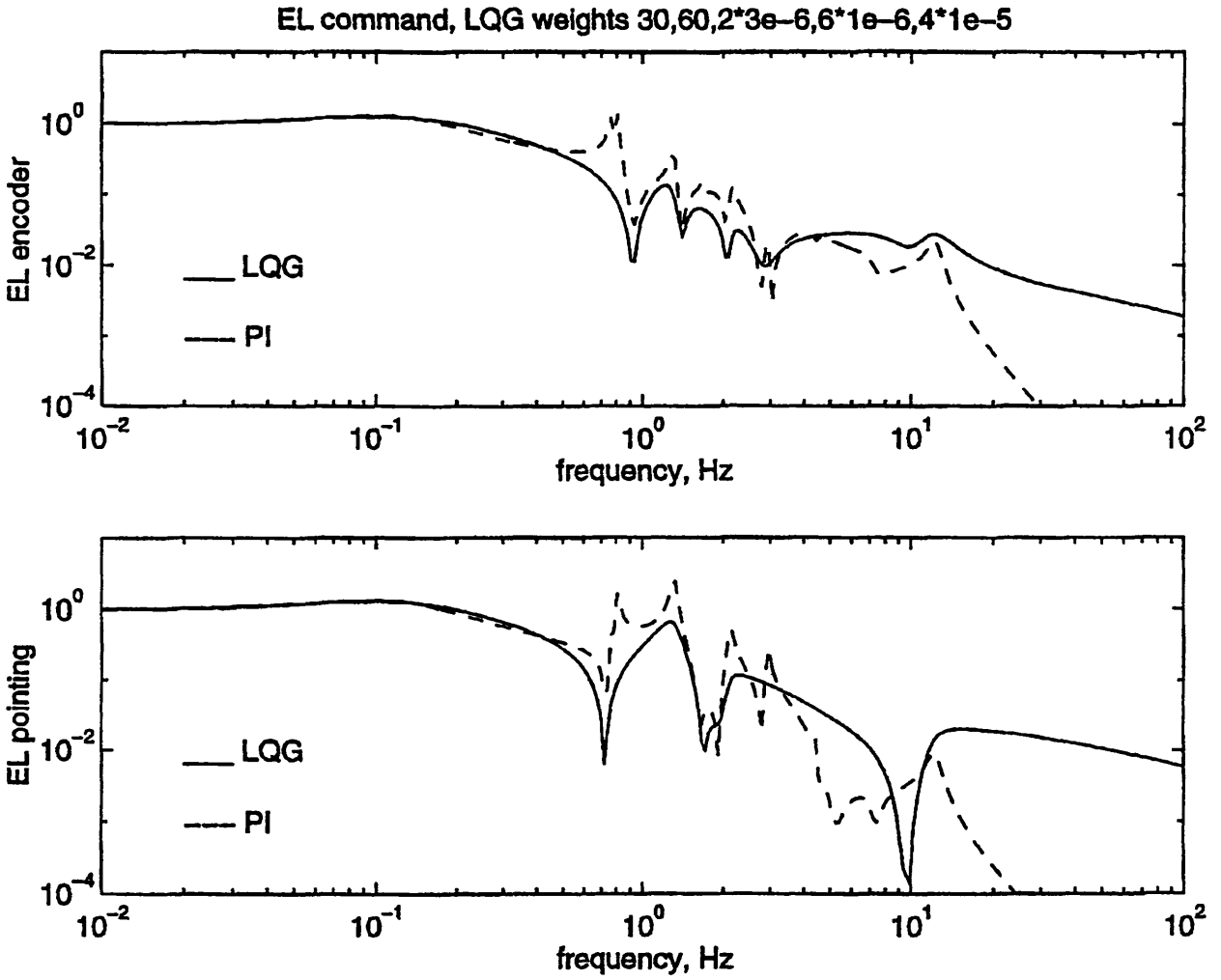


Fig.6 Magnitudes of transfer function: (a) from elevation command to elevation encoder, and (b) from elevation command to elevation pointing.

Fig.6a,b

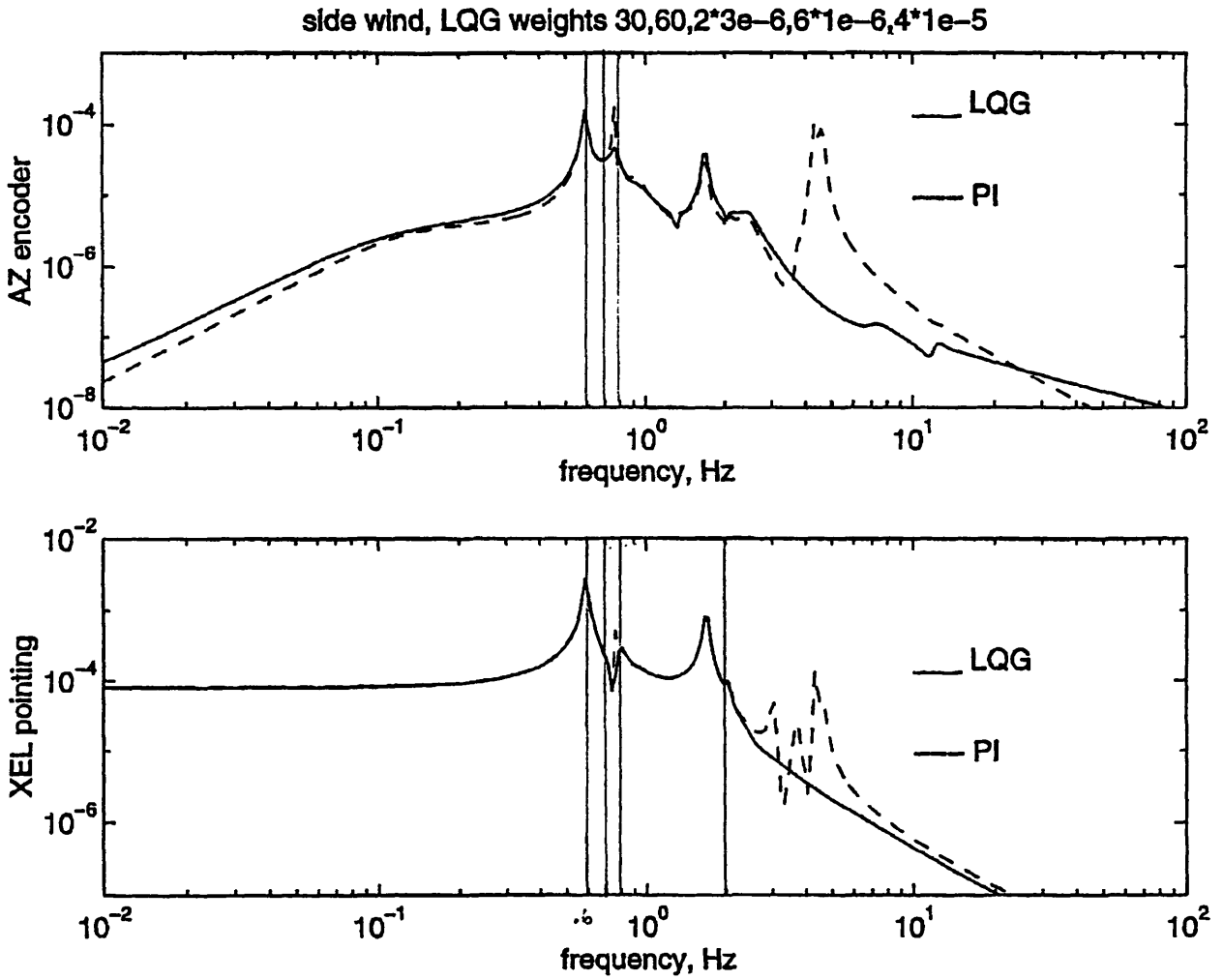


Fig.7 Magnitudes of transfer function from side wind to (a) azimuth encoder and (b) cross-elevation beam.

Fig.7a,b

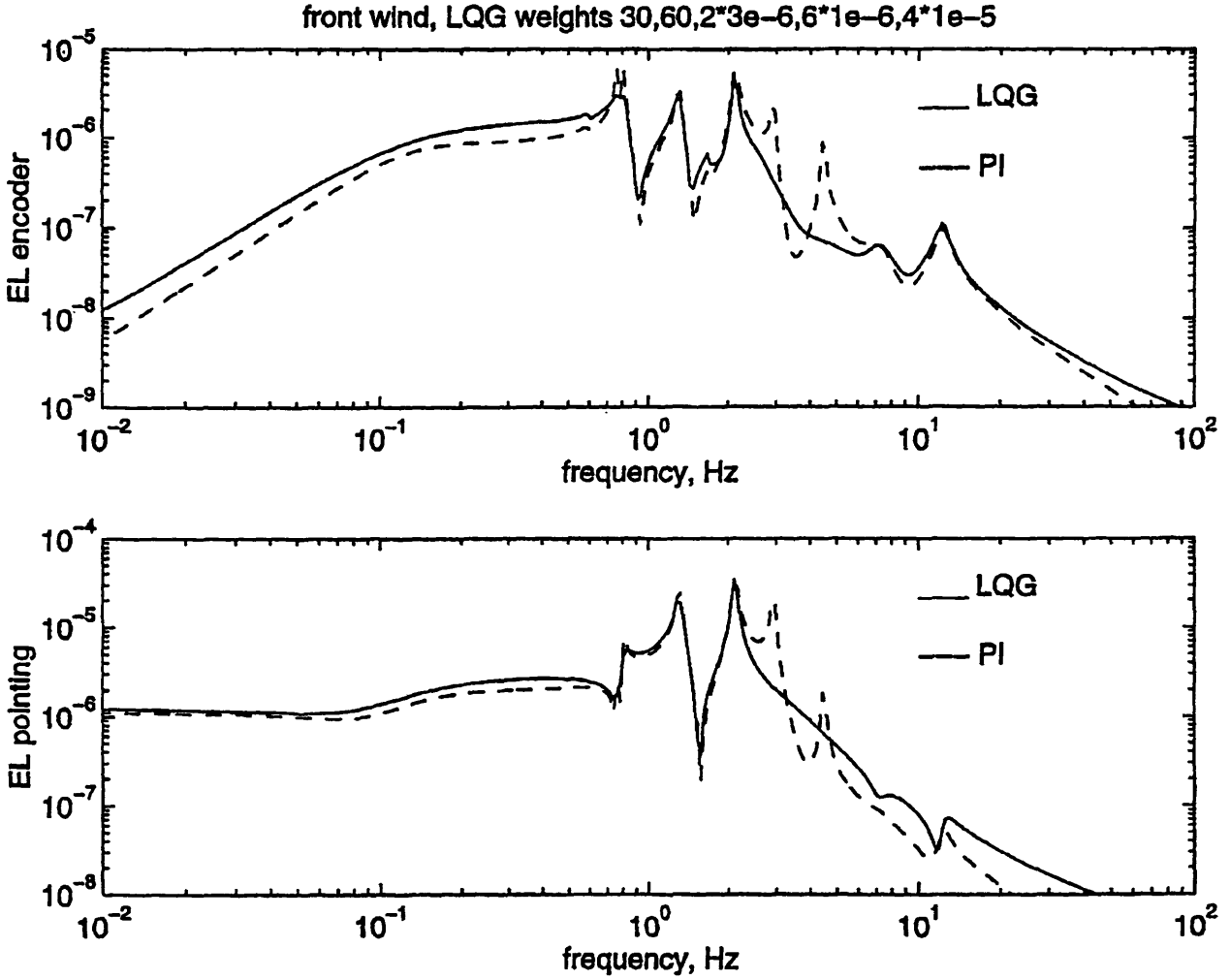


Fig.8 Magnitudes of transfer function from front wind to (a) elevation encoder and (b) elevation beam.

Fig.8a,b